Fisher Waves in the Strong Noise Limit

Oskar Hallatschek[*]

Max Planck Research Group for Biological Physics and Evolutionary Dynamics,
Max Planck Institute for Dynamics & Self-Organization (MPIDS), Göttingen, Germany

K. S. Korolev[†]

Department of Physics and FAS Center for Systems Biology, Harvard University, Cambridge, Massachusetts 02138, USA
(Received 8 May 2009; published 2 September 2009)

We investigate the effects of a strong number fluctuations on traveling waves in the Fisher-Kolmogorov reaction-diffusion system. Our findings are in stark contrast to the commonly used deterministic and weak-noise approximations. We compute the wave velocity in one and two spatial dimensions, for which we find a linear and a square-root dependence of the speed on the particle density. Instead of smooth sigmoidal wave profiles, we observe fronts composed of a few rugged kinks that diffuse, annihilate, and rarely branch; this dynamics leads to power-law tails in the distribution of the front sizes.

Traveling waves are a common phenomenon in many systems that combine diffusion and reaction of particles. Familiar examples are the combustion fronts running through a premixed reactive gas, or the expanding fronts of bacterial colonies. The standard model for these wave-like phenomena is the stochastic Fisher-Kolmogorov-Petrovsky-Piscounov (SFKPP) equation, the simplest non-linear model that blends diffusion, growth, and number fluctuations. It has been used widely in population genetics [1], ecology [2], epidemiology [2], chemical kinetics [3,4], and recently even in quantum chromodynamics [5].

Our current understanding of traveling waves in reaction-diffusion systems is shaped by studies of the SFKPP equation that have focused on the weak-noise regime. The opposite limit of strong noise is relatively unexplored, yet arguably of equal importance. Not only does it occur naturally, when the driving forces of traveling waves are weak [6]; it also unravels fundamentally different and often counterintuitive aspects of the SFKPP equation. The focus of this Letter is on two intimately related questions of how fast these traveling waves move and what their shape is.

Recently, the velocity of a one-dimensional wave has been computed in the strong noise limit with the help of a duality between the SFKPP equation and $A \rightleftharpoons A + A$ reaction-diffusion system [7]. Here, we treat the growth (reaction) term as a small perturbation, and construct a more direct and more powerful method to calculate the speed of the wave than the one used in Ref. [7]. Our technique has three important advantages. First, the perturbation expansion enables us to compute the wave velocity in two dimensions. We find a square-root dependence of the terminal velocity on the particle density. Second, our approach allows studying the shape of the front on time and length scales that are dominated by the noise. We find that, in one dimension, the noise alone can

stabilize the front and limit its diffusive broadening. The front size distribution exhibits power-law tails due to spontaneous creation and subsequent annihilation of new transition regions. Third, the perturbation expansion can be applied to more general models with polynomial reaction terms of higher order.

Without any loss of generality, we discuss the SFKPP equation from the point of view of population genetics, where it is easy to interpret, simulate, and potentially test [6]. In this context, the SFKPP is used to describe how a mutation that increases the growth rate of its carrier spreads through a homogeneous population [1] (see also Ref. [8] for a recent review). In one dimension, the relative abundance $p(t, x) \in [0, 1]$ of a beneficial mutation at time t and position x is described by

$$\frac{\partial p}{\partial t} = D \frac{\partial^2 p}{\partial x^2} + a p(1 - p) + \sqrt{b p(1 - p)} \eta(t, x). \quad (1)$$

The diffusion term is due to the short-range migration of the individuals. The diffusivity D is proportional to the average dispersal distance in one generation. The reaction term, $a p(1 - p)$, accounts for different fitnesses of the mutant and the "wild" type, and the reaction rate $a > 0$ is the difference in their growth rates. The last term on the right-hand side of Eq. (1) describes the sampling error during reproduction, and is commonly referred to as genetic drift or number fluctuations. The strength of the noise $b > 0$ is inversely proportional to the population density, and the (Itô) white noise $\eta(t, x)$ satisfies the following condition: $\langle \eta(t_1, x_1) \eta(t_2, x_2) \rangle = \delta(t_1 - t_2) \delta(x_1 - x_2)$, where $\delta(\cdot)$ stands for Dirac's delta function.

One of the most important predictions of the SFKPP equation is the velocity v of an isolated wave that moves from the left half-space occupied by the mutant into the right half-space occupied by the wild type. The boundary between the half-spaces is assumed to be sharp initially,

$p(0, x) = 1 - \theta(x)$, where $\theta(x)$ is the Heaviside step function. In the deterministic limit ($b = 0$), the wave acquires a stationary shape with exponential tales, and the velocity of the front approaches $v_F = 2\sqrt{Da}$ [1,3]. In the presence of noise, the behavior of the one-dimensional SFKPP is controlled by the dimensionless number $b^2/(aD)$. Surprisingly, even weak noise, $b^2 \ll aD$, gives rise to large corrections to the velocity, $v = v_F - O[\ln^{-2}(1/b)]$ [9], indicating the importance of fluctuations. Here, we access the strong noise regime, $b^2 \gg aD$, by constructing a perturbation expansion in the reaction rate a, while treating the noise term exactly.

Let us define the average instantaneous velocity of the wave as $v = \frac{d}{dt}\langle \int_{-\infty}^{\infty} p(t, x)dx \rangle$, which is consistent with the usual definition in the deterministic limit. We then take the time derivative inside the integral and use Eq. (1) to eliminate $\frac{\partial p}{\partial t}$; after integrating by parts and averaging, we obtain an alternative expression for the velocity,

$$v = a \int_{-\infty}^{\infty} \langle p(t, x)[1 - p(t, x)]\rangle dx, \qquad (2)$$

which relates the wave speed and the second moment of the dynamical field $p(t, x)$.

Note that, to the first order in a, the instantaneous velocity is given by $aI(t)/2$, where the moment $I(t) = \int_{-\infty}^{\infty} \langle 2p(t, x)[1 - p(t, x)]\rangle dx|_{a=0}$ is evaluated in the neutral limit $a = 0$, when neither the mutant nor the wild type have a selective advantage. The neutral model is exactly solvable because the hierarchy of the moment equations closes [8,10]. For the purpose of this Letter, it is sufficient to consider only the two-point correlation function $H(t, x_1, x_2) \equiv \langle p(t, x_1)[1 - p(t, x_2)]\rangle + \langle p(t, x_2)[1 - p(t, x_1)]\rangle$, which is known in population genetics as the average spatial heterozygosity. $H(t, x_1, x_2)$ is the average probability that, at a time t, two individuals sampled at x_1 and x_2 carry different genetic variants. The equation of motion for H is obtained by differentiating its definition with respect to time and eliminating $\frac{\partial p}{\partial t}$ with the help of Eq. (1). Note that the rules of the Itô calculus must be used to properly account for the effects of the noise [8,10]. The result is

$$\frac{\partial H}{\partial t} = D\left(\frac{\partial^2}{\partial x_1^2} + \frac{\partial^2}{\partial x_2^2}\right)H - bH\delta(x_1 - x_2). \qquad (3)$$

An intuitive way to derive Eq. (3) is to follow the lineages of the two sampled organisms backward in time. Then, $H(t, x_1, x_2)$ changes because the individuals migrate, which is represented by the diffusion term, and because they may have a common ancestor, which is represented by the term proportional to the delta function, since such an event is only possible when the lineages meet.

We compute $H(t, x_1, x_2)$ because it has information about the shapes of the wave front and is related to $I(t)$, and thus v, by $I(t) = \int_{-\infty}^{\infty} H(t, x, x)dx$. To this end, we introduce new spatial variables, $\xi = (x_1 + x_2)/2$ and $\chi = $

$x_1 - x_2$, encoding the average position of two sampling points and the distance between them, respectively. After a Laplace transform in t and Fourier transform in ξ, Eq. (3) can then be solved for $\tilde{H}(s, k, \chi) \equiv \int_0^{\infty} dt e^{-st} \int_{-\infty}^{\infty} d\xi e^{-ik\xi} H(t, \xi, \chi)$. For the sharp front initial condition, the solution reads

$$\tilde{H}(s, k, \chi) = \frac{1}{s + Dk^2}\left[\frac{e^{-\sqrt{\frac{s}{2D}+\frac{k^2}{4}}|\chi|}}{\frac{b}{4D} + \sqrt{\frac{s}{2D} + \frac{k^2}{4}}} + \frac{2}{k}\sin\left(\frac{k|\chi|}{2}\right)\right]. \qquad (4)$$

From the definition of $I(t)$, it follows that the Laplace transform of $I(t)$ equals $\tilde{H}(s, 0, 0)$. Performing the inverse Laplace transform, we get $\lim_{t\to\infty} I(t) = 4Db^{-1}$. Equation (2) then implies that the terminal velocity equals $2aD/b$ in agreement with Ref. [7].

Since only the regions with $p(t, x) \neq 0, 1$ contribute to $I(t)$, the finite limit of $I(t)$ as $t \to \infty$ may look counterintuitive because it suggests a finite length of the transition regions. In other words, the noise term alone limits the diffusive widening of the front. Qualitatively, this phenomenon can be understood by noticing that the probability of reaching local fixation ($p = 0$ or $p = 1$) is very large at the tails of the front, so the stationary shape of the front might be maintained by a balance of the diffusive spreading of the genetic variants into each other's territory and their subsequent loss due to number fluctuations (genetic drift).

We analyze this peculiar phenomenon further via particle simulations. Since our perturbation analysis suggests that, on sufficiently small length scales, the wave dynamics can be well approximated by neglecting Darwinian selection, we set $a = 0$ in the simulations. A snapshot of a typical transition region between $p = 1$ and $p = 0$ is shown in the inset of Fig. 1; the transition occurs on a very short length scale set by D/b. The inset also shows the local heterozygosity $h_0(t, \zeta) = 2p(t, \zeta)[1 - p(t, \zeta)]$, which is nonzero only at the kink. The new coordinate ζ is defined such that $\int_{-\infty}^{0} h_0(t, \zeta)d\zeta = \int_0^{\infty} h_0(t, \zeta)d\zeta$; i.e., point $\zeta = 0$ is always in the center of the wave. Such a definition allows us to focus on the shape of the wave by eliminating the diffusion of the front. It is then instructive to characterize the average shape of the wave by $\mathcal{F}(\zeta) = \lim_{t\to\infty}\langle p(t, \zeta)\rangle$ and $\mathcal{K}(\zeta) = \lim_{t\to\infty}\langle h_0(t, \zeta)\rangle$. In contrast to the narrowness of a typical boundary, these *average* characteristics show power-law tails with exponents close to -1 and -2, respectively; see Fig. 1.

The power-law tails of $\mathcal{K}(\zeta)$ and $\mathcal{F}(\zeta)$ can also be inferred from the exact solution for the two-point correlation function given by Eq. (4). One can see that $\tilde{H}(s, k, \chi) = G(s, k)\mathcal{E}(s, k, \chi)$, where $G = 1/(s + Dk^2)$ is the diffusion Green's function, which describes the motion of the center of the wave, and $\mathcal{E}$ describes the evolution of the shape of the wave front. This decomposition implies that the front diffuses with diffusivity D *independent* of the
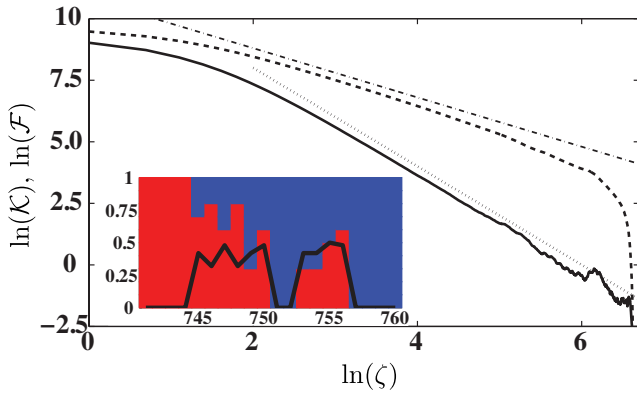
FIG. 1 (color online). Simulation of the neutral one-dimensional stepping stone model [14]. The model considers a line of sites (demes) labeled by an integer j. Each of the demes is occupied by N individuals that carry one of the two genetic variants. Every generation, neighboring demes exchange Nm migrating organisms. Migration is followed by the Wright-Fisher reproduction; i.e., the next generation is formed by N organisms sampled from the Bernoulli distribution with the probability of sampling a particular genetic variant equal to its fraction in the current generation. Here, $N = 10$, and $m = 0.1$; the total number of demes is 1501. We ensure that the wave front remains within the simulated habitat by moving $\zeta = 0$ to the center of the habitat every third generation. The inset shows a snapshot of the wave front $p(t, \zeta)$ [red (lighter) color] and the local heterozygosity $h_0(t, \zeta)$ (solid line) as functions of the deme index j after 10^7 generations starting from the step function initial condition. The main plot shows $\mathcal{F}(\zeta)$ (dashed curve) and $\mathcal{K}(\zeta)$ (solid curve) obtained over 10^8 generations. For large ζ, the functions have the following asymptotic scalings $\mathcal{F}(\zeta) \propto \zeta^{-1}$ and $\mathcal{K}(\zeta) \propto \zeta^{-2}$ shown by dot-dashed and dotted lines, respectively.

noise strength b set by the population density. Furthermore, since factorization in the Fourier and Laplace domains corresponds to convolution in the space and time domains, we can think of $\mathcal{E}(t', \xi', \chi)$ as a contribution to $\tilde{H}(t, \xi, \chi)$ from a wave that was present a distance $\xi - \xi'$ away and time $t - t'$ ago. Power laws in the front size distribution should be reflected in the asymptotic behavior of $\mathcal{E}(t, \xi, \chi)$. We get $\mathcal{E}(t, \xi, \chi = 0) = \frac{\Phi(t)}{\sqrt{2\pi t}} e^{-\xi^2/2t}$ from Eq. (4), where $\Phi(t) = \int_{-\infty}^{\infty} d\xi \mathcal{E}(t, \xi, \chi = 0) \sim t^{-3/2}$ for large times. The new function $\Phi(t)$ is the contribution to H from a transition region present t ago anywhere in space. Since $\int_0^{\infty} dt \mathcal{E}(t, \xi, \chi = 0) \sim \xi^{-2}$ for large ξ, we may conclude that the probability that a kink is located ξ away from the center of the wave should decay like a power law with exponent -2. Indeed, this matches the observed behavior of $\mathcal{K}(\zeta)$ for large arguments.

The algebraic decay of correlations inside a wave front and the slow approach of $I(t)$ to its limit as $t \to \infty$ are in contrast to the narrowness of a typical wave front shown in the inset of Fig. 1. It is unlikely that a single narrow front relaxes so slowly, but several diffusing fronts can exhibit

very slow relaxation, give rise to power-law tails of $\mathcal{K}$ and $\mathcal{F}$, and still have a finite value of $I(t = \infty)$. Indeed, we find spontaneous creation of new kinks in our simulations. This process can be interpreted as the following reaction: $A \rightarrow (2z + 1)A$, where A represents a kink, and z is an integer. Note that the reaction with $z = 1$ is the most frequent. Neighboring kinks can also merge and subsequently disappear, which is equivalent to the annihilation reaction $A + A \rightarrow 0$. Thus the behavior of the front can be described by the dynamics of branching annihilating random walks (BARW) with even number of offspring [11].

For a sufficiently small birth rate, the number of BARW remains finite [11], which is consistent with the finite value of $I(t = \infty)$. Moreover, we can understand the asymptotic behavior of $\mathcal{K}(\zeta)$ and $\mathcal{F}(\zeta)$ by considering the dynamics of only three annihilating random walks (ARW); a higher number of ARW leads to subleading corrections as one can easily show by generalizing our analysis of three ARW. In the ARM picture $\mathcal{K}(\zeta)$ is proportional to the average number of ARW present at position ζ, and $\mathcal{F}(\zeta) \propto \int \mathcal{K}(\zeta) d\zeta \propto \zeta^{-1}$ because, for large ζ, $\mathcal{F}(\zeta)$ is proportional to the probability that the farthest transition region is at least ζ away from the origin.

Since three ARW eventually annihilate, and the process repeats, it is sufficient to consider only one cycle from $A \rightarrow 3A$ to $3A \rightarrow A$. Let $P(t, x_1, x_2, x_3)$ be the probability to find three ARW at time t at positions $x_1 > x_2 > x_3$, which obeys a three-dimensional diffusion equation, with the following absorbing boundary conditions $P(t, x_1, x_2, x_2) = P(t, x_1, x_1, x_3) = P(t, x_1, x_2, x_1) = 0$. Upon using the solution of this diffusion problem from Ref. [12], we obtain $\mathcal{K}(\zeta) \propto \int dt dx_1 dx_2 dx_3 \delta[\zeta - (x_1 - \frac{x_1 + x_2 + x_3}{3})] \times P(t, x_1, x_2, x_3) \propto \zeta^{-2}$. Also note that the survival probability of three ARW $\int dx_1 dx_2 dx_3 P(t, x_1, x_2, x_3) \sim t^{-3/2}$ for long times [12], which matches the behavior of $\Phi(t)$. Thus, on large length scales, the one-dimensional SFKPP equation seems indeed equivalent to a one-dimensional reaction-diffusion system of BARW.

What happens in higher dimensions? The noisy FKPP equation Eq. (1) can easily be extended to two spatial coordinates upon substituting $x \rightarrow \mathbf{r} = (x, y)$, provided one limits the short-wave length variations of the field $p(t, \mathbf{r})$ by a cutoff l, e.g., representing the lattice constant in the model. The speed of a planar wave front traveling in the x direction again takes the form of Eq. (2), and depends on the moment $I(t)$. Solving the two-dimensional neutral version of Eq. (1) yields

$$\tilde{I}(s) = \frac{\sqrt{2D} s^{-3/2}}{1 + \frac{b}{8\pi D} \ln(\frac{32\pi^2 D}{l^2 s})} \qquad \text{(2d)} \qquad (5)$$

for the Laplace transform of $I(t)$. Up to logarithmic corrections, we find that the second moment increases as $I(t) \sim D^{3/2} b^{-1} t^{1/2}$ for long times. Consequently, the wave speed should increase without bound as $v(t) = aI(t)/2 \propto t^{1/2}$, rendering the perturbation expansion sin-
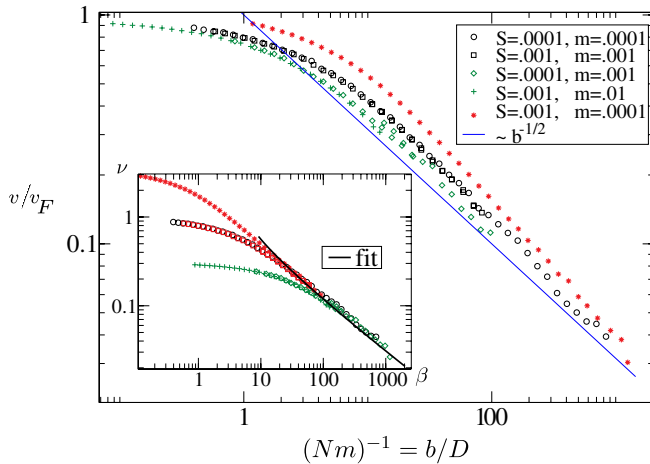
FIG. 2 (color online).   The velocity of planar fronts in the two-dimensional stepping stone model. The simulations are identical to the ones described in Fig. 1 with two exceptions. First, we consider a comoving square lattice of 250×250 sites instead of a linear array. Second, the mutant is $1 + S$ times more likely to reproduce than the wild type. The simulations are initialized by a sharp steplike front profile and run for 2×10^7 generations. The correspondence between the parameters in the simulations and in the SFKPP equation can be expressed as $N = l^2/(b\tau) = 10$, $S = a\tau$, $m = D\tau/l^2$, where l and τ are the lattice constant and the generation time, respectively. For large noise, the wave velocity closely follows a power law $\frac{v}{v_F} \propto (Nm)^{1/2} = D/b$. Deviations are primarily due to log corrections and mimic a power law with an exponent slightly smaller than $-1/2$. Note, the scaling regimes almost collapse in a plot $\nu \equiv (v/v_F)\sqrt{s/m} = (v/v_F) \times \sqrt{al^2/D}$ versus $\beta \equiv (NS)^{-1} = b/(al^2)$, see the inset. The solid line is the solution of $\nu^2 = c_1/[\beta \ln(c_2\nu)]$ with the fitting parameters $c_1 = 0.45$ and $c_2 = 1$.

gular. We circumvent this difficulty by noticing the front does not have enough time to fully relax as predicted by the neutral dynamics. Relaxation only occurs over a limited time t^*, which is roughly the time when deterministic motion of the front is of the same order as its diffusive motion: $vt^* = \sqrt{2Dt^*}$, i.e., $t^* = 2Dv^{-2}$. If this time is large, we may impose a self-consistency condition, $v = 2aI(t^*)$, which leads to the scaling $v \sim D\sqrt{a/b}$ (up to log corrections) for the wave velocity. This heuristic argument, which can be formalized by a multiple-scale ansatz [13], predicts a crossover from the no-noise speed $v \sim 2\sqrt{aD}$ to $v \sim D\sqrt{a/b}$ for large values of the noise strength, $b \gg D$. Simulated wave fronts indeed exhibit this crossover, see Fig. 2.

In conclusion, we have presented a perturbative approach to the one-dimensional SFKPP reaction-diffusion

system with strong number fluctuations, which can be extended to higher dimensions using self-consistency arguments. In one and two dimensions, we found a linear and a novel square-root relationship between the speed of traveling waves and the particle density, respectively. The wave profiles have also been analyzed in one dimension using three different approaches: Simulations, the correspondence between BARW and SFKPP equation, and the exact solution for the two-point correlation function. All of these approaches predict that the front size distribution has a power-law tail with a cutoff, which is in contrast to the exponential tails of deterministic Fisher waves. The power-law tail is best understood as a consequence of spontaneous creation of several transition regions that behave as BARW. Finally, we note that our perturbation expansion also applies to generalized SFKPP equations with higher order polynomial reaction terms. This can be used, for instance, to show that the spread of recessive and dominant beneficial mutations is the same [13].

*ohallats@gmail.com
†papers.korolev@gmail.com

[1] R. Fisher, Ann. Eugenics **7**, 355 (1937).
[2] J. Murray, *Mathematical Biology* (Springer, New York, 2003).
[3] A. Kolmogorov, N. Petrovsky, and N. Piskounov, Moscow Univ. Bull. Math. **1**, 1 (1937).
[4] J. F. Douglas, K. Efimenko, D. A. Fischer, F. R. Phelan, and J. Genzer, Proc. Natl. Acad. Sci. U.S.A. **104**, 10 324 (2007).
[5] C. Marquet, R. Peschanski, and G. Soyez, Phys. Rev. D **73**, 114005 (2006).
[6] J. F. Wilkins and J. Wakeley, Genetics **161**, 873 (2002).
[7] C. R. Doering, C. Mueller, and P. Smereka, Physica A (Amsterdam) **325**, 243 (2003).
[8] K. S. Korolev, M. Avlund, O. Hallatschek, and David R. Nelson, http://arxiv.org/abs/0904.4625v1.
[9] E. Brunet and B. Derrida, Phys. Rev. E **56**, 2597 (1997).
[10] G. Malécot, Theor. Popul. Biol. **8**, 212 (1975).
[11] G. Ódor, Rev. Mod. Phys. **76**, 663 (2004).
[12] M. Fisher, J. Stat. Phys. **34**, 667 (1984).
[13] K. S. Korolev and O. Hallatschek (unpublished).
[14] M. Kimura and G. H. Weiss, Genetics **49**, 561 (1964).